

PPPL-3242 - Preprint: March 1997, UC-427

**TSC Simulation of Feedback Stabilization of
Axisymmetric Modes in Tokamaks using Driven Halo Currents**

S. C. Jardin and J. A. Schmidt

*Princeton Plasma Physics Laboratory
P.O. Box 451,
Princeton, NJ 08543-0451*

December 1996

Abstract

The Tokamak Simulation Code (TSC) has been used to model a new method of feedback stabilization of the axisymmetric instability in tokamaks using driven halo (or scrapeoff layer) currents. The method appears to be feasible for a wide range of plasma edge parameters. It may offer significant advantages over the more conventional method of controlling this instability when applied in a reactor environment.

I. Introduction

Tokamak reactor designs that utilize elongated plasma cross-section shapes require high-power feedback systems to keep the plasma column positionally stable[1]. The conventional design for these feedback systems uses either a dedicated pair of axisymmetric poloidal field coils with up/down asymmetric currents or some combination of the equilibrium shaping coils. The feedback electrical currents in these coils are driven by applying a voltage proportional to a linear combination of the plasma vertical displacement and its time derivative. These poloidal field coils must be located behind the first wall and blanket assemblies in order to avoid excessive neutron capture and heating. The large power required for this system and the associated inductive heating of the cryogenic magnet assemblies cause design problems which set an upper-limit on the practical plasma elongation attainable.

Here we propose and investigate an alternate method [2] for stabilizing the vertical instability utilizing biased electrodes in the vacuum vessel. The electrodes drive a force-free current in the plasma halo, and this current creates a field which acts to stabilize the plasma, resulting in a system with minimal coupling to the cold-structure, and hence reduced recirculating power requirements.

This paper is aimed at demonstrating the principle of halo-current feedback by way of a two-dimensional MHD simulation. In Section II we describe the geometry utilized in our study. It is essentially a tokamak plasma of the ITER[3] shape but with a simplified vacuum vessel geometrical shape in an effort to be more generic. The actual results should be relatively insensitive to the shape of the plasma or the vacuum vessel.

We describe the simulation results in Section III by presenting the results of several parametric studies in Figures 5-8. The results can be understood in terms of a relatively simple circuits model which we present in Section IV. In Section V, we discuss the results and show how they can be readily scaled to other configurations.

II. Configuration

In any axisymmetric system, it is possible to represent the magnetic field as being the sum of a poloidal part obtained from a magnetic flux function and a toroidal part,

$$\vec{B} = \nabla\phi \times \nabla\psi + g\nabla\phi. \quad (1)$$

Here ϕ is the axisymmetry angle, ψ is the poloidal magnetic flux function, and g is the toroidal field function. Consider the idealized system consisting of an axisymmetric tokamak plasma inside an axisymmetric rectangular cross-section vacuum vessel as shown in Figure 1. We divide the plasma inside the vessel into three regions, according to the value of ψ . A high temperature plasma region exists for all magnetic flux values ψ interior to the limiting flux surface ψ_{lim} , ie. for $\psi_{lim} > \psi > \psi_0$, where ψ_0 is the value of ψ at the magnetic axis. The region outside the last closed flux surface is divided into two regions, the halo region with temperature T_H occupying the flux region with $\psi_H > \psi > \psi_{lim}$, and the vacuum region with $\psi > \psi_H$. We define the width of the halo region in terms of the normalized flux increment $W_H = (\psi_H - \psi_{lim})/(\psi_{lim} - \psi_0)$. In the TSC modeling, the vacuum region is treated as a cold resistive plasma with vacuum temperature $T_V \ll T_H$.

In order to detect the vertical motion of the magnetic axis of the plasma, we use the flux values at two fictitious flux loops located at $(R_1, Z_1) = (8.15, 1.95)$ and $(R_2, Z_2) = (8.15, 0.95)$. A feedback poloidal electric field, proportional to the instantaneous difference in the flux values of the two loops, $\delta\psi_{1,2} = \psi(R_1, Z_1) - \psi(R_2, Z_2)$, is applied in the clockwise sense in the upper outboard quadrant of the vacuum vessel. Thus, the poloidal Ohm's law in this upper quadrant of the vacuum vessel with $R > 7.0$ m, and $Z > 1.5$ m is

$$E = \eta J + E_{FB} \quad (2)$$

where η is the vessel resistivity, J is the vessel current density, and $E_{FB} = \alpha \delta\psi_{1,2}$ for some proportionality constant α . The applied poloidal electric field is limited to be less than E_{MAX} in absolute magnitude. Note that over the distance $l_W \approx 8$ m over which it is applied, this would lead to a voltage difference $V = l_W E_{FB}$ in the absence of current. Voltage drops in the sheath at the nelectrodes are neglected in this analysis.

III. Simulation Results

We have modeled the time dependent evolution of this system using the Tokamak Simulation Code (TSC)[4]. The vessel resistivity and thickness are taken to be $\eta = 1.4 \times 10^{-4}$ $\Omega\text{-m}$ and $\Delta = 0.15$ m, corresponding to a L/R decay time of 0.0035 sec. for the first up/down antisymmetric decay mode. A typical TSC run proceeds as follows:

An initial equilibrium configuration is computed with no currents in the vessel or in the halo or vacuum regions. A conventional vertical feedback stabilizer which utilizes PF coils external to the vessel is used during the initial equilibrium iteration to maintain vertical stability during that phase of the calculation. At time zero, this vertical feedback system is disengaged and the system evolves in time according to the two-dimensional (axisymmetric) resistive MHD evolution equations given in Ref. [4-6], which are appropriate for plasma motion slow compared to the Alfven time. The halo-current feedback system is engaged at some subsequent time $t = t_{FB}$, and we model the system motion for a fixed value of T_H , W_H , α , E_{MAX} and T_V .

Figures 2a-b plot contours of the toroidal field function g (see Eq. 1) at a fixed time for two different halo feedback calculations with halo width $W_H = 0.4$ (Fig. 2a) and $W_H = 0.01$ (Fig. 2b). The other parameters for these runs were $T_H = 20$ eV, $\alpha = 266$, $E_{MAX} = 40$ V/m and $T_V = 0.1$ eV. These contours correspond to streamlines for the poloidal current, which is given by $\vec{J} = \mu_0^{-1} \nabla g \times \nabla \phi$. The contours deep inside the plasma region are suppressed in these plots.

We see that for the wide halo case, Fig. 2a with $W_H = 0.4$, the majority of the driven halo current flows through the upper right corner of the vessel, and returns through the plasma halo, with the driven halo current being well aligned with the magnetic field. This is particularly true for that part of the plasma halo that intersects the vessel on both ends. When the halo field lines do not intersect the vacuum vessel on both ends, such as is the case for the inner halo contours on Fig. 2a and for all the halo contours on Fig. 2b, the patterns for the poloidal current contours are somewhat different. Here we see that the poloidal current extends further down and around the main plasma so that the current density \vec{J} is greatly reduced in the region where it crosses the flux surfaces in order to connect the vessel current to the current in the thin halo region. This is particularly evident in Fig. 2b.

The results from a typical run are shown in Figure 3 where we plot the plasma magnetic axis and the applied feedback electric field strength E_{FB} as functions of time. This case corresponded to a run with $t_{FB} = 0.4s$, $T_H = 20 eV$, $W_H = 0.2$, $\alpha = 133$, $E_{MAX} = 10 V/m$ and $T_V = 0.35 eV$. We see from Figure 3b that after an initial transient period of about 0.1 seconds, the Z-position of the magnetic axis begins to move from its initial location Z_0 with exponential time dependence $Z - Z_0 \sim exp(\gamma t)$ with a growth rate of $\gamma \approx 5 s^{-1}$. At $t = t_{FB} = 0.4 s$, the halo-current feedback system turns on with an electric field strength limit of 10 V/m. This system remains limited for about 0.12 s, during which time it has produced halo currents to restore the plasma to its Z_0 location. After this time, the feedback system settles to a lower electric field level needed to maintain the plasma in a position slightly offset from the neutrally stable point. Figure 4 shows the poloidal currents flowing in the 8 m of passive structure where the electric field is applied, with each curve corresponding to a different 15 cm section. The maximum poloidal current passing through any part of the vessel cross section is seen to be less than 0.6×10^6 Amperes.

Studies were done of the effect of the proportionality constant α and of the maximum electric field strength E_{MAX} on the plasma motion. The 5 curves on Figure 5 correspond to the same situation as above except that the gain parameter α takes on the values of 0.000, 33, 66, 133, and 266. In Figure 6 we extend this study to include variation of E_{MAX} . We show the results of calculations with the combinations of (α, E_{MAX}) of (266, 10), (533, 40), and (533, 80).

We have also studied the sensitivity of these results to the plasma properties assumed in the halo region. Figure 7 shows the results of 5 runs with differing values of the halo temperature, T_H , of 1.0 eV, 2.0 eV, 5.0 eV, 10.0 eV, and 20.0 eV. In Figure 8 we see the effects of the halo width, W_H on the plasma evolution. The three runs marked 1-3 correspond to values of W_H equal to 0.01, 0.1, and 0.4. The other parameters for these runs were $T_H = 20 eV$, $\alpha = 266$, $E_{MAX} = 40 V/m$, and $T_V = 0.35 eV$.

Finally, we show in Figure 9 the dependence of the system performance on the vacuum region temperature T_V . Curves 1-3 correspond to values of T_V equal to 5 eV, 0.35 eV, and 0.1 eV. All runs had $W_H = 33$, $T_H = 20 eV$, $\alpha = 266$, and $E_{MAX} = 40 V/m$. We see that while higher vacuum temperatures work best for these narrow halo widths, the system still responds adequately for the lowest vacuum temperatures investigated, $T_V = 0.1 eV$.

We can summarize the results of this sections as follows: The halo current feedback scheme appears to offer a viable method for controlling the vertical instability in tokamaks. The method seems to work for a relatively wide range of parameters characterizing the spatial extent and temperature of the plasma halo region, and of the vacuum region. Larger gain parameters and maximum electric field strengths always work better, as do hotter and wider halo regions. When the halo width is small, hotter vacuum temperatures work better than colder ones. However, none of these dependencies are particularly strong.

IV. Simple Circuits Model

The TSC simulation code solves the full two-dimensional resistive MHD equations as described in detail in Refs. [4-6]. However, for purposes of understanding the results from TSC, it is often useful to develop a simpler analytical model that still contains the essence of the physics. Let us consider the simplified model shown in Figure 10.

The plasma has toroidal current I_P and is free to move rigidly in the Z -direction. The vessel wall has a toroidal current I_W . The halo current is shown in the upper right corner of the figure. For analysis, we divide the path in which the halo current flows into 2 segments as shown. It is purely poloidal (i.e., in the plane of the paper) in the wall (segment 2), but follows the magnetic field lines in the plasma halo region (segment 1) so that it has both a toroidal (i.e., directed into the paper) and a poloidal component.

The equivalent circuit equations for the halo current in segment 2 is obtained from Eq. (2). If we integrate this over the wall volume in the upper-right corner (see figure 10), we obtain expressions for the poloidal resistance and applied feedback voltage in the wall between points A and B:

$$R_{H2} = \eta_W \frac{l_W}{A_W}$$

$$V_2 = \alpha l_W \delta \psi_{1,2}$$

Here l_W is the distance along the wall between points A and B where the halo currents leave and enter the wall, A_W is the wall cross-sectional area to poloidal currents, and η_W is the wall resistance. For region 1, the circuit equations are obtained from the Ohm's law valid in the plasma halo region,

$$\vec{E} + \vec{V} \times \vec{B}_0 = \eta_H \vec{J} \quad (3)$$

Here \vec{B}_0 is the equilibrium magnetic field, assumed to be time independent in this analysis for simplicity. Let $\vec{E} = -\frac{\partial \vec{A}}{\partial t} - \nabla \Phi$ and take the dot product of Eq. (3) with the equilibrium magnetic field \vec{B}_0 ,

$$-\vec{B}_0 \cdot \frac{\partial \vec{A}}{\partial t} - \vec{B}_0 \cdot \nabla \Phi = \eta_H \vec{B}_0 \cdot \vec{J}. \quad (4)$$

In the Coulomb gauge, the vector potential \vec{A} is defined in terms of currents in the plasma, wall and halo (P+W+H) by the Greens's function integral

$$\vec{A}(\vec{x}) = \iiint_{P+W+H} G(\vec{x}, \vec{x}') \vec{J}(\vec{x}') d\vec{x}' \quad , \quad (5)$$

where

$$G(\vec{x}, \vec{x}') = \frac{\mu_0}{|\vec{x} - \vec{x}'|} \quad (6)$$

with μ_0 being the permeability of free space. We also make use of the identity

$$\vec{B}_0 \cdot \nabla \Phi = \nabla \cdot (\vec{B}_0 \Phi). \quad (7)$$

Integrating Eq. (4) over the plasma halo segment 2, bounded by the vacuum vessel at points A and B, yields, after some manipulation,

$$\frac{\partial}{\partial t} (L_H I_H + M_{HP} I_P + M_{HW} I_W) + R_{H1} I_H = \Delta V \quad (8)$$

where ΔV is the electrostatic potential drop between points A and B bounding segment 2 of the halo region. We have also defined the mutual inductance between the halo current and the plasma current, and the halo current and the wall current, and the halo current resistance in segment 1 as follows:

$$M_{HP} = \frac{1}{I_P \iint \vec{B}_0^P \cdot dA} \iiint_H \vec{B}_0^T(\vec{x}) \cdot \iiint_P G(\vec{x}, \vec{x}') \vec{J}(\vec{x}') d\vec{x}' d\vec{x}, \quad (9)$$

$$M_{HW} = \frac{1}{I_W \iint \vec{B}_0^P \cdot dA} \iiint_H \vec{B}_0^T(\vec{x}) \cdot \iiint_W G(\vec{x}, \vec{x}') \vec{J}(\vec{x}') d\vec{x}' d\vec{x} \quad (10)$$

$$R_{H1} = \frac{1}{I_H \iint \vec{B}_0^P \cdot dA} \iiint_H \eta_H \vec{B}_0(\vec{x}) \cdot \vec{J}(\vec{x}) d\vec{x} \quad (11)$$

Note that we have assumed that the amount of poloidal flux in the halo region intersecting the wall is the same at points A and at B in Fig. 10, namely $\iint \vec{B}_0^P \cdot dA$. The total self-inductance of the halo region is the sum of two parts, one due to the toroidal part of the helical halo current in the plasma, and one due to the poloidal halo current in the plasma and the structure.

$$L_H = L_H^P + L_H^T \quad (12)$$

From Amperes' law, the part due to the poloidal current is just given by

$$L_H^P = \mu_0 \iint \frac{dA}{2\pi R} \quad (13)$$

where the integration is over the area inside the halo current path. In analogy with Eqns. (9) and (10), the toroidal part of the self-inductance is given by

$$L_H^T = \frac{1}{I_H \iint \bar{B}_0^P \cdot dA} \iiint_H \bar{B}_0^T(\bar{x}) \cdot \iiint_H G(\bar{x}, \bar{x}') \bar{J}(\bar{x}') d\bar{x}' d\bar{x}. \quad (14)$$

Thus, the final circuits equation for the halo current can be written

$$\frac{\partial}{\partial t} (L_H I_H + M_{HP} I_P + M_{HW} I_W) + R_H I_H = \alpha L_W \Delta \psi_{1,2}, \quad (15)$$

Where we have combined the resistance of the two halo segments into a single halo resistance, $R_H = R_{H1} + R_{H2}$. A linearized form of Eq. (15) is given by

$$L_H \frac{\partial I_H}{\partial t} + M'_{HP} I_P \frac{\partial Z}{\partial t} + M_{HW} \frac{\partial I_W}{\partial t} + R_H I_H = \alpha L \Delta \psi_{1,2}. \quad (15a)$$

The linearized equations for the wall current and the plasma motion are obtained in their normal ways:

$$L_W \frac{\partial I_W}{\partial t} + M'_{WP} I_P \frac{\partial Z}{\partial t} + M_{HW} \frac{\partial I_H}{\partial t} + R_W I_W = 0, \quad (16)$$

and

$$I_P (M'_{PH} I_H + M'_{PW} I_W) + 2\pi R I_P B_R^0 Z = 0, \quad (17)$$

with primes (') denoting differentiation with respect to Z . After replacing time-derivatives by the mode growth rate γ , equations (15a)-(17) can be combined into the single dispersion relation:

$$\det \begin{vmatrix} 1 & m'_{WP} & m'_{HP} \\ m'_{WP} & (1 + \frac{\gamma_W}{\gamma}) & \frac{M_{WH}}{L_W} \\ (\frac{L_W}{L_H} m'_{HP} - \frac{\alpha^*}{\gamma}) & \frac{M_{WH}}{L_H} & (1 + \frac{\gamma_H}{\gamma}) \end{vmatrix} = 0. \quad (18)$$

We have defined $m'_{HP} = M'_{WP} \times (I_P / 2\pi R B_R^0 L_W)^{1/2}$, $m'_{WP} = M'_{HP} \times (I_P / 2\pi R B_R^0 L_W)^{1/2}$, $\gamma_W = R_W / L_W$, $\gamma_H = R_H / L_H$, and $\alpha^* = \alpha L \times (\delta\psi_{1,2} / \delta Z) \times (I_P / 2\pi R B_R^0 L_W)^{1/2} / L_H$.

Equation (18) is of the same form as the dispersion relation analyzed in Ref. [7]. It is quadratic in $1/\gamma$. For physical parameters of interest, both solutions should be damped (stable) for values of the gain parameter α sufficiently large. We thus conclude that the halo-current feedback studied here is very similar in behavior to the more conventional method of active feedback control of the axisymmetric mode studied in Ref.[7]. Even though the halo-current and it's driving voltage are purely in the poloidal direction in the vessel, when they enter the plasma halo, they take on a toroidal component due to the force-free constraint requiring currents to align with the local magnetic field. This toroidal component of the driven plasma

halo current interacts with the other toroidal currents in the system (in the wall and plasma) in a manner very similar to the way in which the toroidal current in a conventional feedback control PF coil does.

V. Summary and Discussion

We have demonstrated that within the confines of our computational model, it is possible to control the axisymmetric instability in non-circular tokamak plasmas by applying a voltage difference, proportional to the plasma vertical displacement, between poloidally separated electrodes in the vacuum vessel. This voltage drives a poloidal current through the vacuum vessel and the plasma halo.

As the current carrying electrons leave the vessel at the electrodes and enter the plasma, they pick up a toroidal component to align with the primarily toroidal magnetic field in the plasma. The toroidal component of the driven plasma halo current provides a radial magnetic field at the plasma such as to restore the plasma vertical position.

We can use this simple picture to estimate how much current in the halo would be needed to restore a typical displacement of the plasma. The radial component of the external magnetic field near the plasma magnetic axis is of order

$$B_R \approx \frac{\mu_0 I_P}{2\pi R} \left(\frac{Z}{R} \right) |n| \quad (19)$$

where I_P is the plasma current, R is the major radius, Z is the vertical displacement and n is the external magnetic field index,

$$n \equiv - \frac{R}{B_Z} \frac{\partial B_Z}{\partial R}.$$

The radial magnetic field at the magnetic axis produced by a halo current at the plasma edge is approximately

$$B_H \approx \frac{\mu_0 I_H^T}{2\pi a},$$

where a is the minor cross section dimension scale and I_H^T is the toroidal component of the halo current. For stabilization, we require $B_H \approx B_R$, or

$$\frac{I_H^T}{I_P} \approx |n| \left(\frac{a}{R} \right)^2 \left(\frac{Z}{a} \right). \quad (20)$$

The ratio of the toroidal to the poloidal halo current is approximately given by

$$\frac{I_H^T}{I_H^P} \approx \Delta\theta \left(\frac{a}{R} \right)^2 \left(\frac{RB_T}{\mu_0 I_P} \right), \quad (21)$$

where $\Delta\theta$ is the poloidal angular extent (in radians) of the halo current in the plasma. Solving Eqns. (20) and (21) for the poloidal halo current gives

$$I_H^P = I_P \left(\frac{\mu_0 I_P}{RB_T} \right) \left(\frac{Z}{a} \right) \left(\frac{|n|}{\Delta\theta} \right). \quad (22)$$

For the geometry studied here, we have $\left(\frac{\mu_0 I_P}{RB_T}\right) = 0.57$, $\left(\frac{Z}{a}\right) = 0.03$, $\Delta\theta = \pi/2$, $|n| = 3$.

Insertion of these values into Eq. (22) gives $I_H^P = 0.03 I_P$ or 6×10^5 Amps., in good agreement with the maximum currents plotted in Fig. 4.

Acknowledgments:

Research sponsored by the Office of Fusion Energy Science, USDOE, under Contract No. DE-AC05-84OR21400.

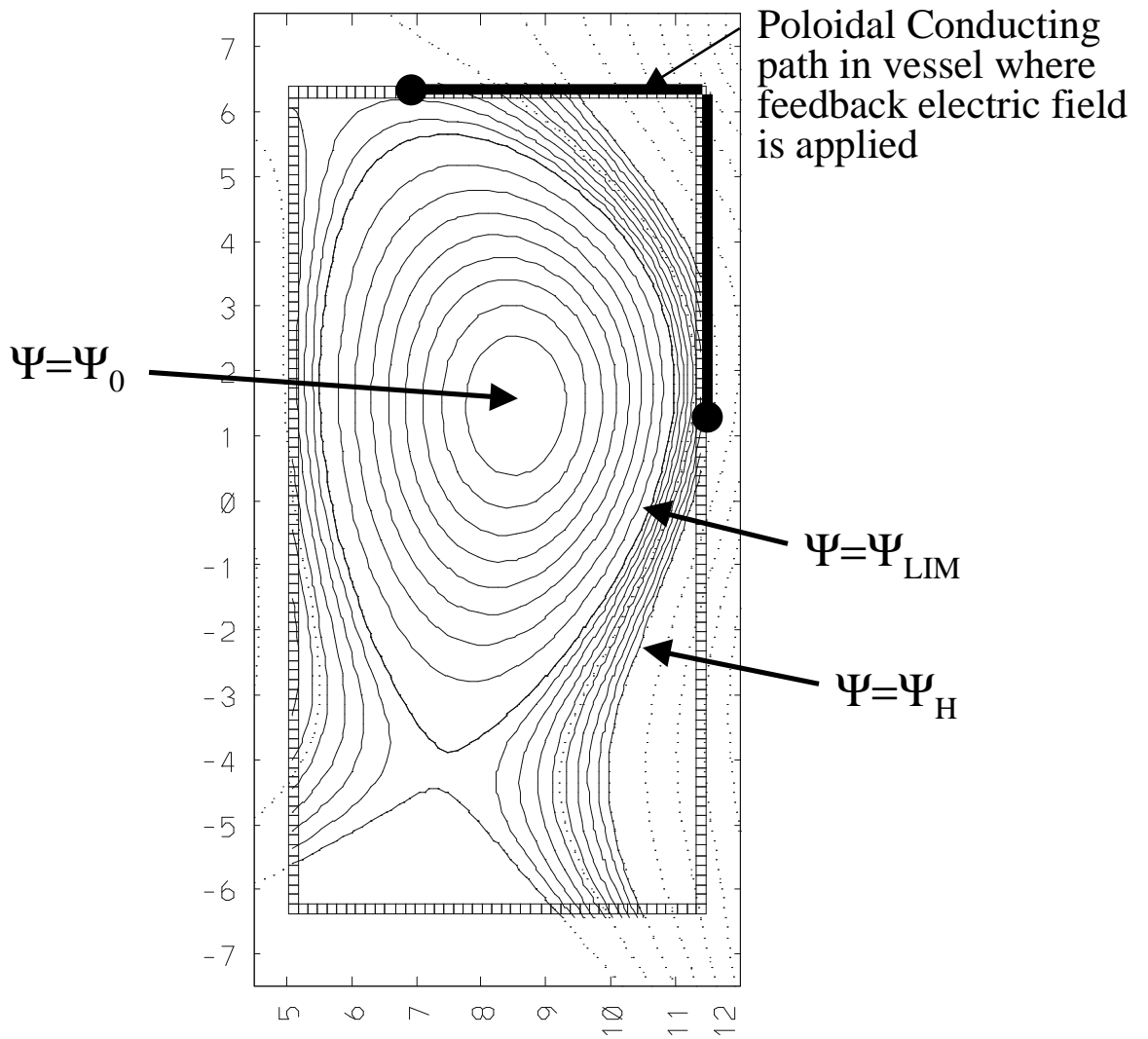
References:

- [1] F.Najmabadi, R. Conn, et al., "The ARIES-I Tokamak Reactor Study", UCLA-1323 (1991)
- [2] Schmidt, J.A., and Jardin, S.C., Bull. Am. Phys. Soc, **41** 1435 (1996)
- [3] Rutherford, P.H., Journal of Fusion Energy, **13** (1994) 83
- [4] Jardin, S.C., DeLucia, J., and Pomphrey, N., J. Comput. Phys **66** 481(1986)
- [5] Sayer, R.O, Peng, Y.M., Jardin, S.C., et. al., Nucl. Fusion **33** 969 (1993)
- [6] Jardin, S.C., Pomphrey, N., and Bell, M, Nucl. Fusion **33** (1993) 371
- [7] Jardin, S.C., Larrabee, D.A., Nucl. Fusion **22** (1982) 1095

Figure Captions

1. The volume inside the vessel is divided into 3 regions: The plasma region, the halo region, and the vacuum region. The upper right corner of the vessel has a voltage difference proportional to the plasma vertical displacement.
2. Poloidal current streamlines at a fixed time for two different halo feedback calculations with halo width $W_H = 0.4$ (Fig. 2a) and $W_H = 0.01$ (Fig. 2b). The other parameters for these runs were $T_H = 20$ eV, $\alpha = 266$, $E_{MAX} = 40$ V/m and $T_V = 0.1$ eV. Streamlines deep inside the plasma region are not shown.
3. A typical feedback stabilization test allows the plasma to move vertically without the feedback system turned on from $t=0$ to $t=0.4$ sec. At $t=0.4$ sec, the halo current feedback system is turned on and the plasma Z-position returns to it's equilibrium location. Plotted are the Z-position of the magnetic axis and the strength of the feedback poloidal electric field as a function of time.
4. Poloidal currents in each of the vessel conductor elements as a function of time for the test shown in Figure 3. When adjacent curves do not overlay, it implies that current is entering or leaving the structure at that point.
5. A test of the sensitivity of the plasma motion to the feedback strength parameter α . Curves marked 1-5 have α values (0, 33, 66, 133, 266). In these runs, $E_{MAX} = 10$ V/m, $W_H = 0.2$, and $T_H = 20$ eV.

6. A test of the sensitivity of the plasma motion to the maximum allowed electric field strength E_{MAX} . Curves marked 1-3 have (α, E_{MAX}) values of $(266, 10)$, $(533, 40)$, and $(533, 80)$. All runs have $W_H = 0.2$, $T_H = 20 \text{ eV}$, and $T_V = 0.35 \text{ eV}$
7. The results of 5 runs with differing values of the halo temperature. Curves 1-5 correspond to values of T_H of 1.0 eV, 2.0 eV, 5.0 eV, 10.0 eV, and 20.0 eV. These runs all had $W_H = 0.2$, $a = 266$, $E_{MAX} = 10 \text{ V/m}$ and $T_V = 0.35 \text{ eV}$.
8. This shows the effects of the halo width, W_H on the plasma evolution. The three runs marked 1-3 correspond to values of W_H equal to 0.01, 0.1, and 0.4. The other parameters for these runs were $T_H = 20 \text{ eV}$, $a = 266$, $E_{MAX} = 40 \text{ V/m}$, and $T_V = 0.35 \text{ eV}$.
9. This series shows the effect of the vacuum resistivity T_V . Curves 1-3 correspond to values of T_V equal to 5 eV, 0.35 eV, and 0.1 eV. All runs had $W_H = .001$, $T_H = 20 \text{ eV}$, $a = 266$, and $E_{MAX} = 40 \text{ V/m}$.
10. Geometry from which to derive simplified circuits model of plasma, wall, halo-system. Poloidal currents are in the plane of the paper, while toroidal currents are into the paper.



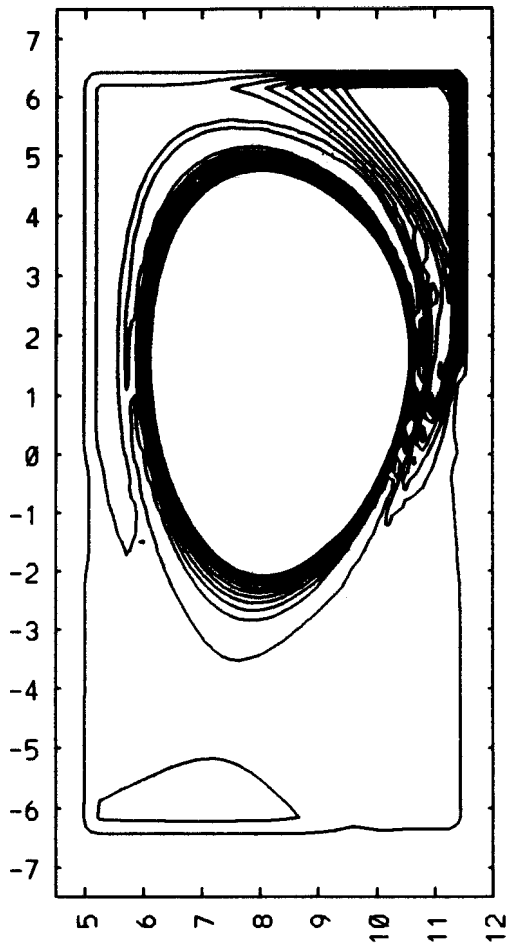


Fig. 2a

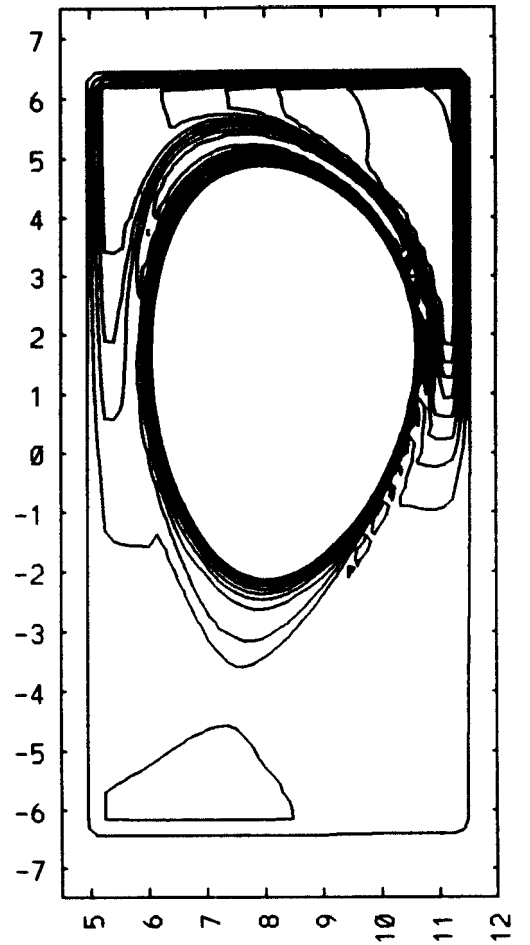


Fig. 2b

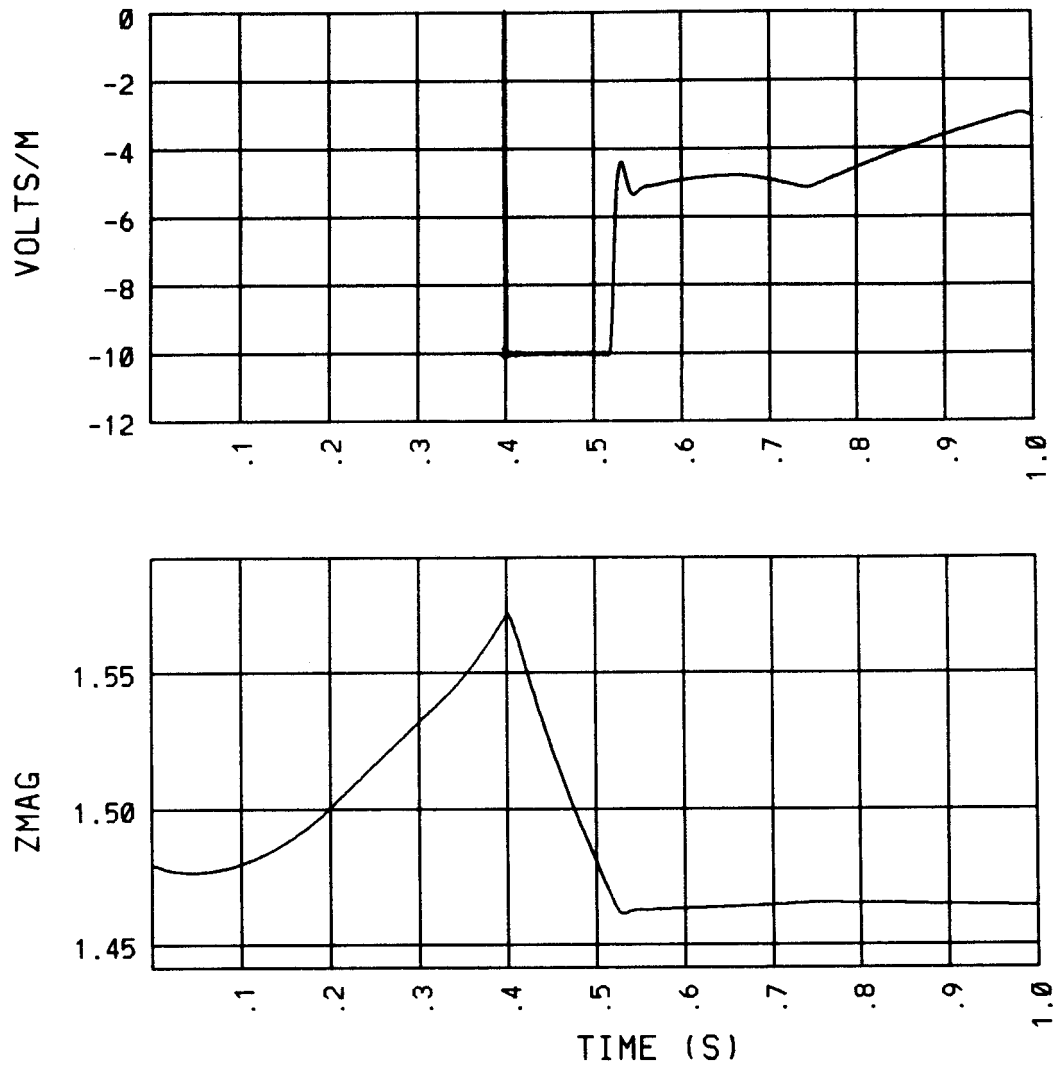


Fig. 3

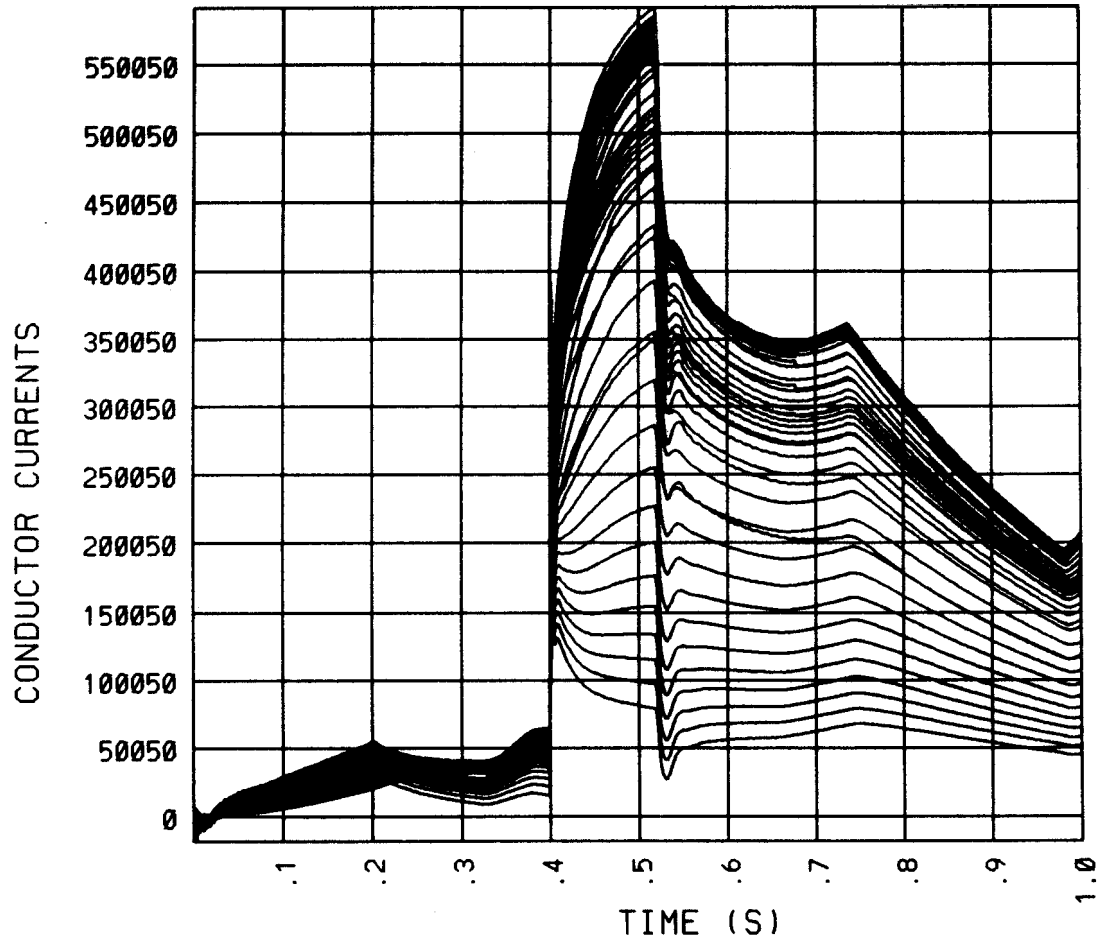


Fig. 4

